Table IV
Limiting Values for N_p-N_s Solutions Used for $D^{(c)}_1$ in Eq 4

N_s, N	$D_{SO_4^{2-}} \times 10^6$, cm²/s 3-3 ionene	6-6 ionene
0.00050	0.26	2.40
0.0010	0.30	3.00
0.0050	0.44	4.66
0.100	1.14	5.68

coefficient of the polyelectrolyte. The higher $D_{1,obsd}$ values for the 6-6 ionene as compared to the 3-3 ionene are believed to be due to a coiling of the more flexible polycation due to divalent counterion condensation. As X is decreased from about $2 < X < 3$ to $X = 0.1$, $D_{1,obsd}$ increases. This is probably due to both the SO_4^{2-} ions in the ionic atmosphere and the condensed SO_4^{2-} ions since the equivalent concentration ratio of salt to polyelectrolyte increases as X decreases. Thus, the tracer and nonradioactive SO_4^{2-} ions are distributed between the polyelectrolyte and the simple salt at low X values according to their weighted concentrations.

It is desirable to obtain the counterion tracer diffusion coefficient for those ions in the ionic atmosphere, for this is a measure of the long-range ion-polyion interaction. For high molecular weight polyelectrolytes with diffusion coefficients very much smaller than those for small ions, the condensed radioactive small ions would not contribute appreciably to the measured counterion tracer diffusion coefficients. If the diffusion coefficient of the polyelectrolyte is *not* negligible compared to that of the counterions and if counterion condensation takes place, then the measured counterion diffusion coefficient $D_{1,obsd}$ is

$$D_{1,obsd} = D^{(c)}_{1,eff} + D^{(u)}_{1,eff} \quad (3)$$

where $D^{(c)}_{1,eff}$ and $D^{(u)}_{1,eff}$ are the effective diffusion coefficients of the condensed counterions and uncondensed counterions, respectively. To determine the desired quantity $D^{(u)}_{1,eff}$, the weighted concentration average of $D^{(c)}_{1,eff}$ is used, i.e., $D^{(c)}_1(1 - (Z_1\xi)^{-1})N_p/(N_p + N_s)$, giving

$$D_{1,obsd} = D^{(c)}_1(1 - (Z_1\xi)^{-1})X/(X + 1) + D^{(u)}_{1,eff} \quad (4)$$

where $D^{(c)}_1$ is the diffusion coefficient of the condensed counterions and hence of the polyelectrolyte. Values of $D^{(c)}_1$ can be obtained from tracer diffusion measurements of divalent (or higher valent) counterions when they are added to a polyelectrolyte whose counterions are monovalent. Recently, direct evidence has been reported[25] that shows that tracer amounts of radioactive Ca^{2+} ion condensed onto sodium heparin, and the values observed for $D_{Ca^{2+}}$ were very close to the values obtained for the tracer diffusion coefficient of the polyelectrolyte itself. Also the replacement of monovalent counterions by trace amounts of divalent and trivalent counterions has been confirmed indirectly from tracer diffusion measurements[7,8,11-16] and from potentiometric measurements.[26,27] In the absence of direct experimental information pertaining to the charge fraction of the ionene halides, an assumption had to be used in eq 4 to evaluate the weighted contribution of counterions dissociated from the polyelectrolyte. The validity of the Manning theoretical charge fraction of the polyelectrolyte was assumed for $\xi > \xi_c$, i.e., $(1 - (Z_1\xi)^{-1})$.[17]

To determine the appropriate values to use for $D^{(c)}_1$ in eq 4, it is noted from Table II that in the range $3 < X < 10$, fairly constant $D_{1,obsd}$ values for SO_4^{2-} are observed. At high X values, where there is an excess of polyelectrolyte to salt, the small amounts of SO_4^{2-} ions replace the condensed Br^- ions, so that the measured diffusion is due to the diffusion of the polyelectrolyte in this region. Then $D^{(c)}_1 = D_{1,obsd}$ in the range $3 < X < 10$. These values are the ones listed in Table IV and are used in eq 4 to calculate $D^{(u)}_{1,eff}$. For comparison with theory the data are also presented as $D^{(u)}_{1,eff}/D^{\circ}_1$, where $D^{\circ}_1 = 1.06 \times 10^{-5}$ cm²/s for SO_4^{2-} ion. With this correction, it should be noted from Tables II and III that below $X = 3$ (excess salt to polyelectrolyte solutions), $D^{(u)}_{1,eff}/D^{\circ}_1$ appears to be fairly independent of salt concentration for each X value, which is predicted by the Manning theory.

Acknowledgment. This project was supported by a grant awarded by the National Science Foundation, DMR77-10237.

Registry No. (1,6-Dibromohexane)·(*N,N,N',N'*-tetramethyl-1,6-hexanediamine) (copolymer), 29322-35-8; 6-6 ionene bromide, 31622-88-5.

References and Notes

(1) Manning, G. S. *J. Chem. Phys.* **1969**, *51*, 924.
(2) Manning, G. S. *J. Chem. Phys.* **1969**, *51*, 934.
(3) Manning, G. S. *Q. Rev. Biophys.* **1978**, *11* (2), 179.
(4) Manning, G. S. *Acc. Chem. Res.* **1979**, *12*, 443.
(5) Manning, G. S. *Biophys. Chem.* **1977**, *7*, 95.
(6) Manning, G. S. *J. Phys. Chem.* **1981**, *85*, 1506.
(7) Magdelenet, H.; Turq, P.; Chemla, M. *Biopolymers* **1974**, *18*, 1535.
(8) Magdelenet, H.; Turq, P.; Chemla, M.; Para, B. *Biopolymers* **1976**, *15*, 175.
(9) Dixler, D.; Ander, P. *J. Phys. Chem.* **1973**, *77*, 2684.
(10) Kowblansky, M.; Ander, P. *J. Phys. Chem.* **1976**, *80*, 297.
(11) Kowblansky, A.; Sasso, R.; Spagnola, V.; Ander, P. *J. Phys. Chem.* **1978**, *10*, 78.
(12) Kowblansky, A.; Gangi, G.; Ander, P. *J. Phys. Chem.* **1978**, *10*, 904.
(13) Silvestri, F.; Leung-Louie, L.; Ander, P. *Macromolecules* **1979**, *12*, 1204.
(14) Ander, P.; Leung-Louie, L. In "Polymeric Amines and Ammonium Salts"; Goethals, E. J., Ed.; IUPAC, Pergamon Press: Oxford, New York, 1980.
(15) Trifiletti, R.; Ander, P. *Macromolecules* **1979**, *12*, 1197.
(16) Magdelenet, H.; Turq, P.; Tivant, P.; Chemla, M.; Menez, R.; Difford, D. M. *J. Chem. Educ.* **1978**, *55*, 12.
(17) Ander, P. In "Solution Properties of Polysaccharides"; Brant, D. A., Ed.; American Chemical Society: Washington, D.C., 1981; ACS Symp. Ser. No. 150.
(18) Anderson, C. F.; Record, M. T., Jr. *Biophys. Chem.* **1980**, *11*, 353.
(19) Kowblansky, M.; Zema, P. *Macromolecules* **1981**, *14*, 166.
(20) Joshi, Y. M.; Kwak, J. C. T. *J. Phys. Chem.* **1979**, *83*, 1978.
(21) Costantino, L.; Crescenzi, V.; Quadrifoglio, F.; Vitagliano, V. *J. Polym. Sci., Part A-2* **1967**, *5*, 771.
(22) Noguchi, H.; Rembaum, A. *Macromolecules* **1972**, *5*, 253, 261.
(23) Rembaum, A.; Baumgartner, W.; Eisenberg, A. *J. Polym. Sci., Polym. Lett. Ed.* **1968**, *6*, 159.
(24) Rembaum, A. *J. Macromol. Sci., Chem.* **1969**, *A3*, 87.
(25) Ander, P.; Lubas, W. *Macromolecules* **1981**, *14*, 1058.
(26) Shimizu, T.; Minakata, A.; Imai, N. *Biophys. Chem.* **1981**, *14*, 333.
(27) Miyamoto, S. *Biophys. Chem.* **1981**, *14*, 341.

Crossover Behavior for the Directed Lattice Animals Model of Anisotropic Polymers†

JOHN M. DEUTCH

Department of Chemistry, Massachusetts Institute of Technology, Cambridge, Massachusetts 02139.
Received May 9, 1983

I. Introduction

Recently, Daoud et al.[1] have examined the collapse and phase separation of linear and randomly branched polymers by a scaling analysis. In this note, the analysis of

† Supported in part by the National Science Foundation.

these authors is extended to so-called directed lattice animals,[2] which speculatively may serve as a model for composite polymeric materials. The free energy is constructed so that the polymer tends to align as a linear chain in the $R_\parallel$ direction and as a randomly branched polymer in the remaining $d - 1$ directions.

The mean field free energy for the model anisotropic polymer under consideration is

$$\frac{F}{kT} = \frac{R_\parallel^2}{a^2N} + \frac{R_\perp^2}{a^2N^{1/2}} + \frac{vN^2}{R_\parallel R_\perp^{d-1}} + \frac{wN^3}{R_\parallel^2 R_\perp^{2(d-1)}} \quad (1)$$

where N is the number of segments of length a in the polymer and $v(w)$ denotes the interaction energy between pairs (triples) of monomers.

In a *good* solvent, $v > 0$ and minimization of the free energy with respect to $R_\parallel$ and $R_\perp$ leads to the results of Redner and Coniglio[3]

$$R_\parallel \sim N^{\nu_\parallel} \quad (2a)$$

$$R_\perp \sim N^{\nu_\perp} \quad (2b)$$

with

$$\nu_\parallel(d) = (d + 11)/[4(d + 2)] \quad (3a)$$

$$\nu_\perp(d) = 9/[4(d + 2)] \quad (3b)$$

The critical dimension is $d_c = 7$, above which the polymer adopts its classical conformation, $\nu_\parallel = {}^1/_2$ and $\nu_\perp = {}^1/_4$.

In a *poor* solvent, $v < 0$ and $w > 0$, the polymer collapses, and we find

$$\nu_\parallel = \nu_\perp = 1/d \quad (4)$$

At T_Θ, the Θ point, $v = 0$ and $w > 0$. In this case, one finds[3]

$$\nu^\Theta{}_\parallel(d) = (d + 7)/[4(d + 1)] \quad (5a)$$

$$\nu_\perp(d) = 3/[2(d + 1)] \quad (5b)$$

with $d_c = 5$.

II. Crossover Behavior in the Θ Region

We proceed to apply the crossover scaling analysis of Daoud et al.[1] in the Θ region. One assumes the Θ region is approached according to $v \sim \tau$, with $\tau = |T - T_\Theta|/T_\Theta$. The crossover region is defined by the condition that the repulsive term $vN^2/R_\parallel R_\perp^{d-1} \sim 1$. Accordingly, for small τ, we must have $\tau \sim N^{-\phi}$. An expression for the crossover exponent ϕ is determined by replacing $R_\parallel$ and $R_\perp$ by eq 2 but with use of the Θ-point exponents in eq 5. One finds

$$\phi(d) = 2 - \nu^\Theta{}_\parallel - (d - 1)\nu^\Theta{}_\perp = (d + 7)/[4(d + 1)] \quad (6)$$

For $d = 3$ this predicts $\tau \sim N^{-5/8}$, in contrast to the result[1] for a linear chain, $\tau \sim N^{-1/2}$, and for the branched chain, $\tau \sim N^{-11/16}$.

The crossover in the transition region is determined by

$$R_\alpha = N^{\nu^\Theta{}_\alpha} f_\alpha(|\tau|N^\phi) \qquad \alpha = \parallel, \perp \quad (7)$$

where $f_\alpha(z) \to z^{x_\alpha}$ for large z. The exponent x_α is determined by the condition that in the collapsed state $R_\alpha \sim N^{1/d}$ according to eq 4. The result for the collapsed state is

$$R_\parallel = N^{1/d}\tau^{-[(d+4)(d-1)/d(d+7)]} \quad (8)$$

and

$$R_\perp = N^{1/d}\tau^{-[2(d-2)/d(d+7)]} \quad (9)$$

For $d = 3$ the predictions are $R_\parallel \sim N^{1/3}|\tau|^{-7/15}$ and $R_\perp \sim N^{1/3}|\tau|^{-1/15}$, in contrast to the result[1] for a linear chain, $R \sim N^{1/3}|\tau|^{-1/3}$, and for the branched chain, $R \sim N^{1/3}|\tau|^{-5/33}$.

An identical procedure leads to results for transition into the good solvent region. The result is

$$R_\parallel = N^{\nu_\parallel}\tau^{(3d-7)/(d+2)(d+7)} \quad (10)$$

and

$$R_\perp = N^{\nu_\perp}\tau^{3(d-1)/(d+2)(d+1)} \quad (11)$$

where $\nu_\parallel$ and $\nu_\perp$ are given by eq 3. For $d = 3$ the predictions are $R_\parallel \sim N^{7/10}\tau^{1/25}$ and $R_\perp \sim N^{9/20}\tau^{3/10}$, in contrast to the result for a linear chain, $R \sim N^{3/5}\tau^{1/5}$, and for a branched chain, $R \sim N^{1/2}\tau^{1/11}$.

III. Simple Prediction for Coexistence Curve

Daoud et al.[1] also propose a simple argument for determining phase separation for linear and branched polymers. For the anisotropic polymer considered here the coexistence curve of τ vs. monomer concentrations is determined by assuming that phase separation occurs when the volume fraction $\phi = c/NR_\parallel R_\perp^{d-1}$ reaches some constant. Use of eq 8 and 9 leads to the curve

$$\tau \sim c^{(d+7)/[3(d-1)]} \quad (12)$$

For $d = 3$ the prediction is $\tau \sim c^{5/3}$, compared to the classical result[1] for the linear chain, $\tau \sim c$, and for the branched chain, $\tau \sim c^{11/5}$. Note that according to eq 12 at the critical dimension $d_c = 5$, one regains the classical result $\tau \sim c$.

IV. Transition to Isotropic Single-Chain Behavior

The transition from directed polymer behavior to isotropic single-chain behavior can be examined by the method of Daoud and Joanny.[4] One modifies the mean square radius of gyration in the denominator of the transverse elastic energy in eq 1 only. In the second term on the right-hand side of eq 1, the expression for the square radius of gyration for a random network where branching occurs at every step $[a^2N^{1/2}]$ is replaced by the expression when there are, on the average, n segments between branching sites $[a^2(nN)^{1/2}]$. Minimization of the free energy leads to

$$R_\parallel = aN^{\nu_\parallel}n^{(1-d)/[4(d+2)]} \quad (13a)$$

$$R_\perp = aN^{\nu_\perp}n^{3/[4(d+2)]} \quad (13b)$$

In the limit $n \to N$, one approaches single-chain behavior $R_\parallel \sim R_\perp \sim aN^{3/(d+2)}$ and $d_c \to 4$.

One can also employ a "blob" picture[1,4,5] to determine $R_\parallel$ and $R_\perp$ for $4 < d < 7$. If the blobs of monomer are considered to consist of n segments of size ξ, one may write

$$R_\parallel = \xi(N/n)^{\nu_\parallel} \quad (14a)$$

$$R_\perp = \xi(N/n)^{\nu_\perp} \quad (14b)$$

For $4 < d < 7$, one expects ideal blob behavior $\xi = an^{1/2}$, and one finds

$$R_\parallel = aN^{\nu_\parallel}n^{(d-7)/[4(d+2)]} \quad (15a)$$

$$R_\perp = aN^{\nu_\perp}n^{(2d-5)/[4(d+2)]} \quad (15b)$$

Evidently $R_\parallel = R_\perp aN^{1/2}$ for $n \to N$. For $d < 4$ one expects swollen blobs $\xi = an^{3/d+2}$ and the result eq 13 is regained. Similar arguments can be constructed to examine the transition to pure branched behavior and transitions at the Θ point.

V. Conclusion

In this note, we have shown how scaling arguments may be applied to the mean field theory model of directed

lattice animals to describe crossover behavior in the Θ region, phase separation, and crossover behavior to isotropic single chains.

References and Notes

(1) M. Daoud, P. Pincus, W. H. Stockmayer, and T. Witten, *Macromolecules*, in press.
(2) S. Redner and Z. R. Yang, *J. Phys. A: Math Gen.*, **15**, L177 (1982), and references cited therein.
(3) S. Redner and A. Coniglio, *J. Phys. A: Math. Gen.*, **15**, L273 (1982).
(4) M. Daoud and J. F. Joanny, *J. Phys. (Orsay, Fr.)*, **42**, 1359 (1981).
(5) P.-G. de Gennes, "Scaling Concepts in Polymer Physics", Cornell University Press, Ithaca, NY, 1979.

Communications to the Editor

Processable, Oriented, Electrically Conductive Hybrid Molecular/Macromolecular Materials

Significant advances have recently been made in understanding and modifying the properties of electrically conductive molecular[1] and macromolecular solids.[1,2] Nevertheless, many of these substances exhibit limitations with regard to chemical/structural control at the molecular level, mechanical stability, air, water, and temperature stability, solubility and processability, and ease of synthesis. In the present communication, we address some of these limitations and describe an approach to the formation of a new class of hybrid molecular/macromolecular solids that can be spun into flexible, oriented, electrically conductive fibers.[3] The approach capitalizes upon similar solubility characteristics yet complementary electrical and structural properties of a well-characterized, chemically flexible, dopable "molecular metal" and a robust, processable, and in this case orientable, macromolecule. Although we illustrate with phthalocyanine molecular conductors[4,5] and a high-modulus "aramid" polymer,[6] the approach would appear to have considerable generality.

Metallophthalocyanines (A) and Kevlar[6] (B) are soluble

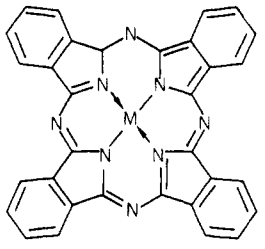

A

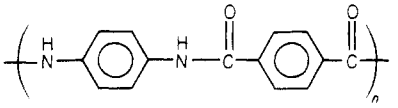

B

in strong acids. Partial oxidation of the former with a variety of electron acceptors results in highly conductive solids (e.g., Ni(Pc)I: σ(crystal) $\approx$ 500 Ω^{-1} cm^{-1}, σ(powder) $\approx$ 5 Ω^{-1} cm^{-1} at 300 K),[4,5] while the latter forms liquid crystalline solutions[6,7] which can be wet-spun[8] into strong, crystalline, highly oriented fibers.[6] Thus in a typical experiment, solutions of vacuum-sublimed phthalocyanine (e.g., Ni(Pc) and H_2(Pc), 5–18% by weight) and Kevlar-29 (3–7% by weight) were prepared in trifluoromethanesulfonic acid at 80 °C under an inert atmosphere. Fibers were then wet-spun from this viscous solution by extrusion under pressure[3,9] (through a stainless steel syringe needle) into an aqueous precipitation bath. Halogen oxidants[4] such as iodine can be introduced into the spinning solution prior to extrusion (presumably promoting more homogeneous doping) or into the precipitating bath (as I_3^-), or alternatively, the washed and dried fiber can be immersed in a benzene solution of I_2. In the latter two procedures, the extrudate is exposed to halogen for at least 24 h prior to washing and drying. Additionally, fibers can be doped electrochemically.[10] The resulting, darkly colored fibers are qualitatively strong and flexible[11] (decreasing flexibility with increasing M(Pc) content) and, as judged by appearance, mechanical properties, and transport properties (vide infra), are stable to air and moisture for many months. The composition of the fibers was established by elemental analysis.[12]

Table I
Electrical Conductivity Data for Hybrid Phthalocyanine/Keylar Fibers

composition[a]	σ_{RT},[b] Ω^{-1} cm^{-1}	act. energy,[c] eV
$[Ni(Pc)(K)_{4.36}I_{1.66}]_n$[d]	1.4	11.4×10^{-3}
$[Ni(Pc)(K)_{1.58}I_{1.27}]_n$[d]	1.8	6.6×10^{-3}
$[Ni(Pc)(K)_{0.67}I_{1.07}]_n$[d]	2.5	12.0×10^{-3}
$[Ni(Pc)(K)_{0.43}I_{1.56}]_n$[e]	4.7	17.2×10^{-3}
$[H_2(Pc)(K)_{0.54}I_{1.24}]_n$[d]	1.2	13.4×10^{-3}

[a] Pc = phthalocyaninato; K = Kevlar monomer unit = $-COC_6H_4CONHC_6H_4NH-$ (B). [b] Four-probe measurement; RT = 300 K. [c] From least-squares fit to the equation $\sigma = \sigma_0 e^{-\Delta/kT}$. [d] Doping in C_6H_6/I_2. [e] Doping in aqueous KI/I_2 followed by electrochemical oxidation (10 V, 3 h) in 0.8 M aqueous HI.

Electrical conductivity measurements were made by standard four-probe dc, techniques.[5a-c] Blocking electrode measurements established that ion conduction is not significant, while control studies (without M(Pc)) verified that the Kevlar host, which absorbed negligible halogen, is an insulator. M(Pc)/Kevlar fibers prepared without oxidation are also insulators. Charge transport data are compiled in Table I, and representative variable-temperature plots are shown in Figure 1A. The conductivity conforms approximately to thermally activated behavior, and phenomenological "activation energies" obtained by linear regression analysis of ln σ vs. $1/T$ plots are given in Table I. However, more satisfactory fits (especially at lower temperatures) are obtained to eq 1[5a,13] (Figure 1B), sug-

$$\sigma = \sigma_0 e^{-[T_1/(T+T_0)]} \quad (1)$$

gestive of transport involving inhomogeneous mixtures of metallike and nonconductive structural regimes with fluctuation-induced carrier tunneling between parabolic barriers separating the metallike regions.[5a,13] Maximum conductivities of the present fibers are on the order of ca. 5 Ω^{-1} cm^{-1}, which compares favorably with many conventional filled polymer composites.[14]

0024-9297/84/2217-0260$01.50/0